

# **Detecting Ash Middens using Remote Sensing techniques: a comparative study in Southern Gauteng, South Africa**

**Mncedisi Jabulani Siteleki**

**464867**



**Master of Science in Geographical Information Systems and Remote Sensing**

**School of Geography, Archaeology and Environmental Studies**

**Faculty of Science**

**University of the Witwatersrand**

**September 2016**

**Supervisors: Prof. Karim Sadr and Dr Stefania Merlo**

## **Abstract**

The Iron Age is a very critical aspect of South Africa's history. It represents a technology that laid a solid foundation for the development of South Africa in terms of its economy, politics and society. It is therefore imperative to study Iron Age, or rather its remnants such as stone-walled structures and ash middens because these give insight into this critical time period's technology and those responsible for it. Remote sensing spatial technology provides the opportunity not only to study these Iron Age remnants but to save time and resources while doing so through satellite imagery. This study employs remote sensing by comparing different multispectral satellite images– GeoEye 1 and SPOT 5 – to find the optimum platform to detect key archaeological remnants – ash middens – from the Iron Age period in the Suikerbosrand Nature Reserve located in Southern Gauteng, South Africa. The performance of GeoEye 1 and SPOT 5 in detecting ash middens was compared through supervised classification techniques, Support Vector Machine and Maximum Likelihood Classification, on different band combinations of the two images. Overall, the band combination of Green, Red and NIR is the best performing on both SPOT 5 and GeoEye 1 compared to Green, Red, and Mid IR on SPOT 5 and Green, Red, and Blue on GeoEye 1. However, higher accuracy of results for the detection of ash middens were obtained on the GeoEye 1 platform. The GeoEye platform performed better than the SPOT platform in the detection and analysis of ash middens.

**Key Words:** Ash Middens, GeoEye, Remote Sensing, Satellite Imagery, SPOT

## **Declaration**

I hereby declare that this research project is my own work except where I have clearly stated otherwise. I have followed the necessary conventions in referencing the thoughts and ideas of others

Signature: \_\_\_\_\_ Date: \_\_\_\_\_

## **Acknowledgements**

Super thanks to my supervisors Prof. Karim Sadr and Dr Stefania Merlo for all the guidance through-out this project. It was not easy but we pulled through. Many thanks to the University of the Witwatersrand, and the National Research Foundation (NRF) for financial support. Many Super Thanks to my family, the Siteleki clan, for all the love and support through-out my studies.

## Table of Contents

<b>1. Introduction</b> .....	<b>1</b>
1.1. Study Area.....	2
1.2. Problem Statement .....	2
1.3. Conceptual Framework: Research Questions .....	4
1.4. Aims .....	4
1.5. Objectives .....	4
<b>2. Literature Review</b> .....	<b>5</b>
<b>2.1. Archaeology and Iron Age</b> .....	<b>5</b>
2.1. Remote Sensing in Archaeology .....	8
<b>3. Methods and Materials</b> .....	<b>11</b>
3.1. Data Collection: Remote Sensing .....	
3.2. Image Pre-processing .....	12
3.3. Data Analysis Methods .....	13
3.3.1. Classification and Bands .....	14
3.3.2. Accuracy Assessment .....	16
<b>4. Results</b> .....	<b>18</b>
4.1. Classification .....	18
4.2. Accuracy Assessment and Kappa Coefficient .....	23
4.3. User and Producer Accuracy .....	24
4.4. Band Combinations .....	25
<b>5. Discussion</b> .....	<b>26</b>
5.1. Accuracy Assessment and Kappa Coefficient .....	26
5.2. Platforms and Techniques .....	27
5.3. User and Producer Accuracy.....	28
5.4. Bands and Spectral Profiles .....	29
5.5. Limitations .....	29
<b>6. Conclusion</b> .....	<b>30</b>
<b>7. References</b> .....	<b>32</b>
<b>8. Appendix</b> .....	<b>37</b>

## List of Figures

Figure 1: Study area map in Suikerbosrand Nature Reserve, Southern Gauteng, South Africa.

Figure 2: An example of how an arbitrary line was drawn across the image on the Geoeye platform.

Figure 3: An example of how an arbitrary line was drawn across the image on the SPOT platform.

Figure 3: Top: SPOT 5 MLC. Bottom: SPOT 5 SVM. Bands Green, Red, and NIR.

Figure 5: Top: GeoEye 1 MLC. Bottom: GeoEye 1 SVM. Bands Green, Red, and NIR.

Figure 6: Top: SPOT 5 MLC. Bottom: SPOT 5 SVM. Red, Green, and Mid IR bands.

Figure 7: Top: GeoEye 1 MLC. Bottom: GeoEye 1 SVM. Red, Green, and Blue bands.

Figure 8: Confusion matrix of the same bands on the different satellite images, Spot 5 and GeoEye 1

Figure 9: Confusion matrix of different bands on the different satellite images, Spot 5 and GeoEye 1

Figure 10: Left: SPOT 5. Right: GeoEye 1. Profiles from same bands on both platforms: Green, Red, and NIR.

Figure 11: Profiles based on different bands on SPOT 5 and GeoEye 1. Left: SPOT 5 bands: Red, Green, and Mid IR. Right: GeoEye 1 bands: Red, Green, Blue.

## List of tables

Table 1: Major spectral regions used in remote sensing

Table 2. SPOT 5 properties (adapted from [www.spotimage.com](http://www.spotimage.com))

Table 3. GeoEye 1 properties (adapted from [www.digitalglobe.com](http://www.digitalglobe.com))

Table 4: Land cover class

## 1. Introduction

The no longer extant Iron Age societies of Southern Africa dating to the 1700s left traces that, when studied, can provide meaningful glimpses into the past to help the reconstructing of the history of past societies. Remnants of stone-walled structures and ash middens – defined in archaeology as piles of rubbish or ash heaps (Renfrew and Bahn, 1991; Boeyens and Hall, 2009; Boeyens and Plug, 2011) – are critical examples of these traces. Remnants of ash middens, for instance, provide a profound reflection on the political and economic life ways of Iron Age societies. These have been detected and studied at a number of Late Iron Age sites in South Africa, such as Molokwane (Maggs, 1976; Pistorius, 1992; Huffman, 2007), Marothodi and Kadithswene (Boyens 2003, and other references on his study of ash middens) According to Boeyens and Hall (2009) and Boeyens and Plug (2011) the larger the midden, the richer and more powerful was the court that produced it. As a consequence, locating such middens and studying their position within the overall configuration of Iron Age settlements is crucial for the understanding of power relations inside it. Identifying and mapping these ash middens with traditional survey techniques can be difficult, due for example to dense vegetation, and time consuming. The use of multispectral satellite imagery classification offers the potential to speed up the process of detecting them on the ground and to provide a method that will not be so heavily affected by inter-analyst variability in visual identification from panchromatic imagery (as is the case in aerial photo interpretation). The purpose of this research is thus to use visually identify middens on the satellite images. Analysing ash middens on two remote sensing platforms (SPOT 5 and GeoEye 1 satellite imagery) and integrating a ground based approach of ground truthing will give way to improve the detection and therefore study of ash middens.

Studying ash middens sheds light into societies of the past and their complex settlement, political and economic dynamics. The use of remote sensing techniques can provide a platform for effective and efficient research regarding ash middens; in turn, saving money and time often spent during traditional field survey. This research is critical because if the remote sensing platforms perform well (statistically) and produce successful results that answer the research questions, less time and money will be spent in the field, therefore reducing the labour intensiveness that goes into archaeological research. Regardless of the outcome, this research project is a step towards showing the ability of remote sensing to

contribute to archaeological research. In principle, middens can be easily recognizable on the ground. Nevertheless, it takes a lot of walking and spending time to cover ground that can be remotely surveyed in a few minutes with remote sensing.

### **1.1. Study Area**

This research was conducted in the southern Gauteng region of South Africa, where stone-walled structures together with related ash middens are present within what is now known as the Suikerbosrand Nature Reserve (Figure 1). Suikerbosrand lies between the Vaal River and the city of Johannesburg (Sadr and Rodier, 2012) and is predominantly covered by hills and valleys that extend over more than 80km<sup>2</sup> of land (Mason, 1986). The area experiences about 650 -700mm of average annual rainfall, with open grasslands (Mason, 1986; Sadr and Rodier, 2012). Circa 1 000 or more Iron Age settlements are mostly located on the hills and the steep valleys on the southern-western and north-western parts of Suikerbosrand (Mason, 1986). This research focused on a 49 hectare area, which extends a little over Suikerbosrand to an adjacent farm, which was particularly selected for its richness of stone-walled settlements (SWS) and ash middens.

### **1.2. Problem Statement**

Sadr and Rodier (2012) have shown that SWS in the Southern part of Gauteng are easily visible but can be difficult to classify with satellite imagery (remote sensing platforms). Moreover, inter-analyst differences, the variability that exists in identifying and demarcating SWS by different analysts who are interpreting the same set of imagery, in classification play a role in delineating these types of archaeological traces (Hunt and Sadr, 2014). Although the ash middens (and their spatial limits) are not so difficult to identify when conducting field survey; a sharp line to circumscribe them cannot be drawn since the ashy soil around the ash middens gradually fades over a few meters into the background soil. It is important to be able to delineate a line around the ash midden because it allows one to estimate the size of the midden in question. When the ashy soil gets mixed up with the background soil, it becomes somewhat difficult to tell them apart (although it is still).

The introduction and use of remote sensing, as well as the enhancement of satellite imagery (and its characteristics) has had profound advantages for archaeology and its various

applications such as settlement discovery and distribution (MacQuilkan and Sadr, 2010; Abrams and Comer, 2013; Sadr, 2015). These advantages include:

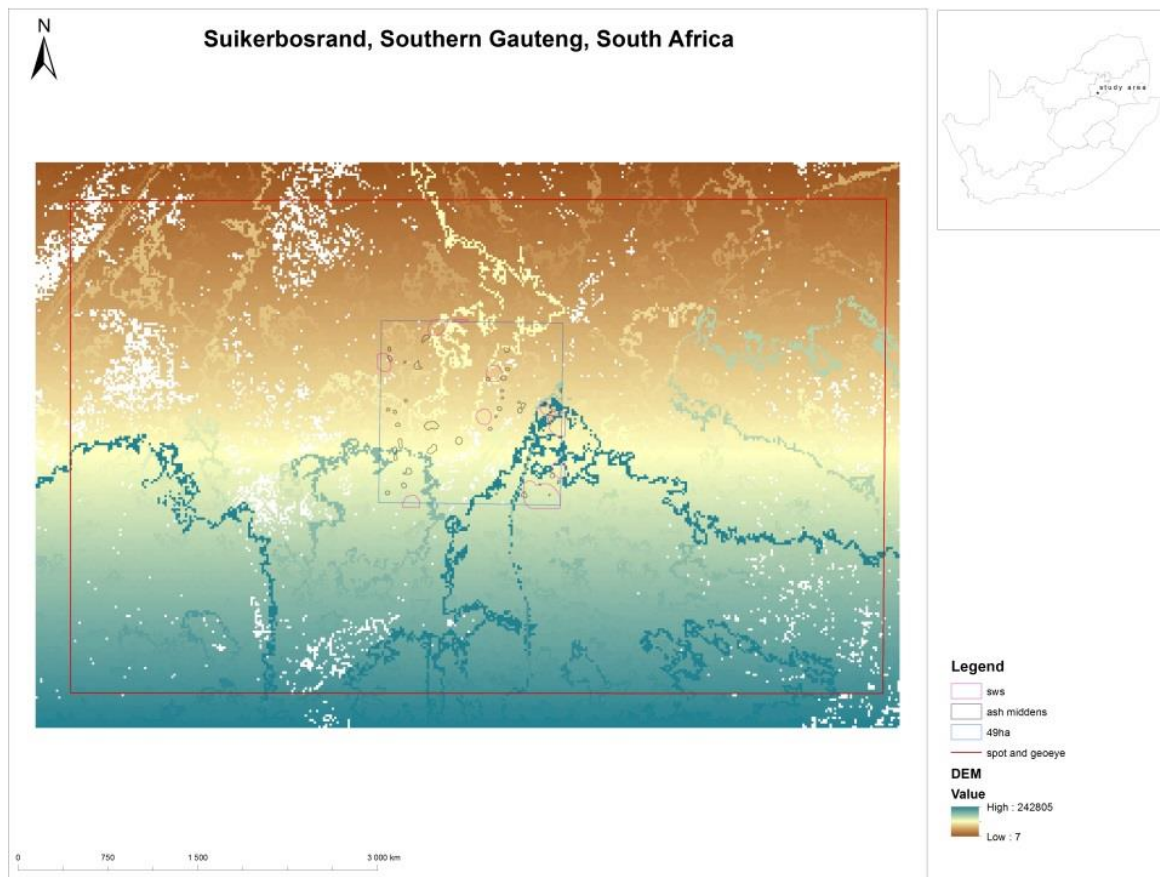


**Figure 1: study area map in Suikerbosrand Nature Reserve, Southern Gauteng, South Africa**

i) its speed which reduces costs, time and the potential risk associated with archaeological survey and excavations; ii) the establishment of site strategies that speak to conservation and preservation (Lasaponara and Masini, 2011). More specifically, in southern African archaeology, remote sensing has inspired and directed scholars to quite comprehensive discussions and conclusions with regards to the people and their settlements (Seddon, 1968; Denbow, 1979; Mason, 1986). For instance, Mason (1865) identified 998 sites in the Transvaal through aerial photographs; Mason (1976) surveyed the highveld identifying settlement patterns; Sadr and Rodier (2012) were able to map and study the evolution of SWS covering an area of over 70,000 square km in southern Gauteng. This would have simply not have been possible through the sole employment of traditional field survey methods due to the sheer amount of data present in the study areas considered.

Consequently, techniques must be established for archaeology so as to better extract and understand information from the various active and passive satellite data sets. The use of statistical techniques is one strong and reliable approach in archaeological research. Sadr and Rodier (2012) employed a statistical approach to identify and analyse the clusters of the vast number of different SWS sites in the Suikerbosrand Nature Reserve; Sadr in press (2012) used statistics to compare, in detail, the SWS group (I, II, and III) structures in the Southern Gauteng region. The understanding of radiometric or geometric distortions, noise reduction and data integration has not been discussed extensively (Lasaponara and Masini, 2011). This is because archaeology has leaned to photo interpretation as a result of the wide use of aerial photography. Therefore, the use of multispectral imagery at high (GeoEye 1) and medium (SPOT 5) resolution brings a new approach in the study of archaeological materials and settlements. The comparison of these sets of imagery will be a crucial initial step towards saving money and time while effectively studying ash middens and better contextualise SWS which otherwise end up being understood as stone wall configuration patterns with little or no archaeology in between.

### **1.3. Conceptual Framework: research question**

For the purpose of this research, two inter-related questions set the core of the study. These questions are:

- Do ash middens have a distinctive spectral signature that allows for their detection in multispectral remote sensing imagery?
- How does the accuracy and precision of supervised classification of ash middens compare at different multispectral imagery resolutions?

### **1.4. Aims**

- To classify archaeological sites (i.e. ash middens) using high and medium multispectral resolution imagery.
- To assess the performance of different remote sensing classification algorithms applied to different multispectral images in detecting ash middens in Southern Gauteng, Southern Africa.

### **1.5. Objectives**

- Identify ash middens (and their extent) on the GeoEye and SPOT images through supervised image classification techniques, Maximum Likelihood Classification (MLC) and Support Vector Machine (SVM)
- Compare and analyse the results and examine their reliability using accuracy assessment.

## **2. Literature Review**

### **2.1. Archaeology and Iron Age**

Social questions are fundamental in studying early societies. They help in exploring the complexities, which include economy, politics and others, that exist (or do not exist) in societies. In archaeology, it is invariably the case that only remnants of these societies are left behind and do not say anything on their own. Social questions therefore need to be asked in an attempt to understand these remnants, and they include: size/scale of the society in question, its internal organisation, politics and socio-economic dynamics (Renfrew and Bahn, 1991). These questions are not meant to make generalizations about societies because of the distinctness and uniqueness that exist in societies such as hunter-gatherers (the San in Southern Africa, for example) and politically complex societies such as Mapungubwe in Southern Africa (Huffman, 2007: 376). Although most of these societies are extinct, they are still worth studying because they give a trace of human behaviour in the past which is rich and holds the potential to provide useful insight for projecting into the future (Fagan, 1992).

Pre-colonial farming societies (also referred to as Iron Age societies) thrived in some parts of Southern Africa, in places like South Africa, Zimbabwe and Botswana. In the interior of South Africa, they extend over Gauteng to North West and farther (Maggs, 1976; Huffman, 2007; Boeyens and Hall, 2009). These farming communities were given the term Iron Age because they made iron tools (Mason, 1974; Huffman, 2007). According to Mason (1974: 211), Iron Age, within a South African perspective, refers to “a technology that led to the earliest major transformation of human society in South Africa”. This technology, based on farming and metal production, laid a solid foundation and paved the way for the booming production of complex technology, economy, politics and societies in South Africa (Mason, 1974). Unlike foragers, these farming communities maintained residence in particular locations for longer time periods. Late Iron Age settlements are characterised by stone-

walled structures with houses and cattle kraals. Middens and storage pits were distributed outside the settlements (Maggs, 1976; Mason, 1986; Hall, 2000; Hall, 2010; Huffman, 2007: 3).

The South African interior is filled with stone-walled structures such that it is difficult, but not impossible, to assign historical identity of the sites to a particular people (Maggs, 1976; Boeyens and Plug, 2011) due to misinterpretations and ignored oral records (Boeyens and Plug, 2011). Nevertheless, it has been established that the (Western) Sotho-Tswana groups are responsible for SWS, known as Molokwane, which occurs over Gauteng to Zeerust, dating from the beginning of the late 18<sup>th</sup> century (Hall, 2000; Huffman, 2007: 38). Sotho/Tswana people, one of Late Iron Age farming communities, extended their settlement buildings south of the Vaal River over the eastern and northern grasslands of the Free State by the early first half of the 17<sup>th</sup> century (Hall, 2010) from north Broedestroom Early Iron Age. Historic records have helped archaeologists identify the presence of Sotho-Tswana groups (from parts of the west) known as the Kwena in the Suikerbosrand (Huffman, 2007: 433).

David (2013: 2) defines ash middens as “rubbish dumps, containing a high proportion of materials considered inedible or not otherwise immediately usable by humans, beasts and poultry”. In contrast, in the interior of South Africa, Tswana communities have various phrases associated with middens such as *‘Kgosi ke thutubudu’* which translates ‘the chief is a midden’ and *‘Kgosi thothobolo e olelwa matlakala’* which literally translates ‘A chief is like an ash-heap on which is gathered all the refuse’. This is interpreted, within a cultural context, as ‘the higher the position, the greater the responsibility’ (Boeyens and Plug, 2011: 9). Researchers such as Hall, Huffman (2007), Mason (1974), Taylor (1979) make the general presumption that the elite of highest rank or senior leader of the village in farming communities possesses the largest household hence has great wealth (Mason, 1986; Boeyens and Plug, 2011), also so as to accommodate all village activities, house a big family and officials (Huffman, 2007: 22). The size of ash middens reflects the size of the political court and its wealth. Consequently, larger court middens mean reflect more feasts as a result of wealth and power. All this combined together is indicative of the political power of the chief. These translations immediately highlight that ash middens in the South African interior are associated with chieftaincy and status.

One important aspect of ash middens entails understanding whether they are just rubbish heaps are related to near-by activities such as religious ceremonies, meals and craftwork (Boeyens and Plug, 2011). In Sukur (Nigeria), various structures that are enclosed within one SWS such as huts/houses or granaries use one midden which is usually located 'outside and close but not immediately next to the entrance of the SWS' (David, 2013). In some Southern African areas, two ash middens are distinguished: large and domestic middens. Large middens are associated with the chief and ruling elite while domestic ones are those related to households (Huffman, 2007; Boeyens, 2009; Boeyens and Plug, 2011). The discarded material from the chief is dumped outside his house, in front of and adjacent to the gateway at its side (Hall, 2000; Boeyens and Plug, 2011). According to David (2013), middens do not really grow in size or age but contribute as nutrients to plots surrounding the house, which is not necessarily the case in South Africa (Boeyens and Plug, 2011). Middens from different areas in the settlement contain just about the same material which includes: organic related material such as ash, bone, fragments, charcoal from hearths (Mason, 1986; David, 2013). This material is a result of economic, religious, juridical and socio-political activities where the elite ruling party of men participated, as well as animal slaughter during public rituals, ceremonies and feasts (Boeyens and Plug, 2011). Activities were in the form of performing very crucial economic dealings and operations; settling high court cases, debates around important political issues (Boeyens, 2009; Boeyens and Plug, 2011). They are also associated with, or a consequence of, the practices of craftwork such as hide-working.

Being able to estimate the sizes and boundaries of ash middens gives significant insight in the life ways of Iron Age societies because large middens are strongly associated with chieftaincy and the elite while smaller ones point to relatively smaller households. Estimates of certain ash middens can be easily used to determine the status or rank of surrounding settlements (whether they belonged to the elite/ senior leaders or not). Furthermore, the relation between settlements and middens might also be made even when the stone-walled structures are no longer visible on the landscape. Remote sensing can contribute to understanding the relations between settlements and ash middens. Detecting and calculating the details of ash middens can in turn inform about the settlements and social, political and economic organization of Iron Age communities.

## 2.1. Remote Sensing in archaeology

Remote sensing techniques offer the opportunity to detect archaeological sites in their complexity and context through satellite imagery. Developments in earth observation techniques over time have provided profound enhancements in landscape studies which mainly include: aerial photographs (AP) for mapping the distribution of stone-walled structures, particularly in the 1960s and 1970s in South Africa (Taylor, 1979; Mason, 1986; Sadr and Rodier, 2012) and Botswana (Seddon, 1968; Denbow, 1979); the use of satellite imagery such as Thematic Mapper in the 1980s (Lasaponara and Masini, 2011), Google Earth (GE) and spatial technologies such as GIS (MacQuilkan and Sadr, 2010; Sadr and Rodier, 2012). However, the use of AP and GE has some limitations which include lack of availability (since AP are often not free) and the unequal resolution of GE through time which means that not all areas in question are covered by the same imagery resolution (MacQuilkan and Sadr, 2010). Moreover, often times archaeological sites and remains are either not clear or hidden from view due to modern vegetation, environmental processes, burial by modern infrastructure (Parcak, 2009). Further advancements in spatial remote sensing techniques have provided new platforms in the form of sensors for acquiring better results through capturing and analysing detailed data.

Advanced remote sensing platforms in the form of passive and active sensors have inspired novel approaches in studying archaeological material. The launch of advanced passive and active sensors as well as multispectral and hyperspectral imagery that have different properties has thus allowed for more complexity in studying archaeological features (Abrams and Comer, 2013). Satellite imagery at high spatial resolution has immensely improved the study of archaeological remains since 1999 (Lasaponara and Masini, 2011). The increase in spectral and spatial resolution of satellite imagery has nevertheless not completely solved the problem of detecting archaeological features. For example, small archaeological material concealed by dense vegetation is still sometimes difficult to study (Lasaponara and Masini, 2011).

Passive sensors, as the ones used to acquire the images in this research rely on natural energy sources, mainly the sun, whereas active sensors make use of their own energy sources which are man-made (Janssen and Bakker, 2004; Woldai, 2004; Abrams and Comer, 2013). Passive sensors, such as SPOT and GeoEye, invariably capture data during the day as

they require the reflected radiation. They are affected by their dependence on the sun, which has changing conditions throughout the day. Atmospheric conditions which interfere with radiation also affect passive sensors. These limitations in turn temper with the detail and complexity within which archaeological features are analysed (Sadr and Rodier, 2012). Passive sensors still provide good ground coverage with relatively good (medium) spatial resolution between 2 and 20/30m with SPOT (Lasaponara and Masini, 2011), Landsat 8 and RapidEye, for example (Toth and Jozkow, 2016). Conversely, high resolution images less than 2m or between 0.31 and 2m include Worldview and IKONOS ([www.seos-project.eu](http://www.seos-project.eu); [www.satimaigingcorp.com](http://www.satimaigingcorp.com)). The use of passive based sensors comes with having to pay careful attention to interferences from the atmosphere which requires the use of specific techniques (i.e. atmospheric correction) before analysing the data.

In remote sensing spatial, spectral and temporal resolutions are distinguished, and differ as per sensor. The definitions used here are adopted from Abrams and Comer (2012: 64): spatial resolution is defined as pixel sizes that belong to satellite imagery or instruments that record image /radiation data, for instance high spatial resolution is 0.41–4 m, and 30-1000 m is low resolution (Digital Globe, 2015); spectral resolution refers to the magnitude of the wavelength interval (bands) that the sensor is measuring, where high spectral resolution is 220 bands, medium is 3-15, and low resolution is 0-3 bands (Digital Globe, 2015); temporal resolution is taken to refer to the time that passes when a sensor acquires image data on particular location, high temporal resolution is <24-3days, medium is 4-16 days, and low is > 16 days (Digital Globe, 2015). Spatial, spectral and temporal resolutions determine the level of detail and complexity within which archaeological features are observed and analysed.

One can see that using different remote sensing techniques allows for analysing the middens on distinct resolutions – spatial, spectral and temporal (Abrams and Comer, 2013). For instance, using active and passive sensor platforms to analyse ash middens may produce different results. This is because spatial and spectral properties will differ depending on the satellite imagery. The naked-eye can only extend vision in the visible portion of the electromagnetic spectrum (see Woldai, 2004: 59 and Parcak, 2009) thus remote sensing is needed as it registers data going beyond this portion (Parcak, 2009). Hence different satellites record reflected radiation in various parts of the electromagnetic spectrum in

different ways (Woldai, 2004). These parts include: the optical portion, the ultraviolet portion which is practically useful for remote sensing, and the visible region (Woldai, 2004: 58). Table 1 (Schowengerdt, 2007: 8) shows spectral regions that are usually used in remote sensing. As a result, greater clarity is perceived by the naked eye as all data beyond the visible electromagnetic spectrum have been recorded, with all distracting features eliminated (Parcak, 2009). Furthermore, this results in clearer and easier reconstruction of past landscapes. All of the above mentioned rigorous processes and techniques ensure that no destruction of the landscape and archaeology within will occur – if any at all – given that archaeological sites tend to be sensitive and therefore minimal disturbance.

Table 1: Major spectral regions used in remote sensing (adapted from Schowengerdt, 2007: 8)

Name	Wavelength range	Radiation source	Surface property of interest
Visible (V)	0.4 – 0.7 $\mu\text{m}$	Solar	Reflectance
Near InfraRed (NIR)	0.7 – 1.1 $\mu\text{m}$	Solar	Reflectance
Short Wave InfraRed (SWIR)	1.1 – 1.35 $\mu\text{m}$ 1.4 – 1.8 $\mu\text{m}$ 2 – 2.5 $\mu\text{m}$	Solar	Reflectance
MidWave InfraRed (MWIR)	3 – 4 $\mu\text{m}$ 4.5 – 5 $\mu\text{m}$	Solar, thermal	Reflectance, Temperature
Thermal or LongWave InfraRed (TIR or LWIR)	8 – 9.5 $\mu\text{m}$ 10 – 14 $\mu\text{m}$	Thermal	Temperature
Microwave, radar	1 mm – 1m	Thermal (passive), Artificial (active)	Temperature (passive), Roughness (active)

It is worth noting that the spatial resolution of satellite imagery can be insufficient to identify and measure objects in their full complexity and detail, looking at shape for instance (Schowengerdt, 2007). This can be somewhat a problem in archaeology, for example, where interest lies in the complexity, detail and full context of discovered objects (Hall, 2000; Huffman, 2007; Sadr and Rodier, 2012). Spectral measurements therefore come into play as they provide an opportunity to identify these objects not exclusively based on their shape but on other characteristics which are a reflection of other (physical and chemical) properties of archaeological remains. Spectral reflectance curves which can be deduced from objects or earth's surface materials indicate radiation that is reflected as a function of wavelength (Woldai, 2004; Schowengerdt, 2007). These reflectance curves are very useful

as they are not just estimates but are specifically related to particular objects (Woldai, 2004).

### 3. Methods and Materials

The data and materials employed in this research project were integrated to produce a balanced remote sensing and ground based project. The remote sensing platforms that were used include: passive sensors SPOT 5 and GeoEye 1 satellite imagery (see tables 1 and 2 for properties of the sensors).

#### 3.1. Data Collection: Remote Sensing

The study area imagery of the various remote sensing platforms were not difficult to access as this research is part of an on-going project on analysing SWS in southern Gauteng (courtesy of Prof. Karim Sadr). The use of different satellite imagery allowed for a comparison between the performances of two passive sensors (GeoEye and SPOT) with different spatial resolutions and comparable spectral bands. The images were acquired during the winter season: June of 2013 for GeoEye 1 and August 2013 for SPOT 5.

**Table 1. SPOT 5 properties (adapted from [www.spotimage.com](http://www.spotimage.com))**

MODE	SPATIAL RESOLUTION (METERS)	SPECTRAL RESOLUTION (MICRONS)
PANCHROMATIC	2.5 – 5	480 – 710 nm
MULITSPECTRAL	10	500 – 590 nm (green)
	10	610 – 680 nm (red)
	10	780 – 890 nm (Near IR)
	20	1.580 – 1.750 nm (Mid IR)

**Table 2. GeoEye 1 properties (adapted from [www.digitalglobe.com](http://www.digitalglobe.com))**

MODE	SPATIAL RESOLUTION	SPECTRAL RESOLUTION
PANCHROMATIC	41 cm GSD at Nadir	450 – 800 nm (black and white)
MULITSPECTRAL	1.65 cm GSD at Nadir	450 – 510 nm (blue)
	1.65 cm GSD at Nadir	510 – 580 nm (green)
	1.65 cm GSD at Nadir	655 – 690 nm (red)

	1.65 cm GSD at Nadir	780 – 920 nm (Near IR)
--	----------------------	------------------------

Ground confirmation is critical regardless of the advantages that come with using remote sensing. It is fundamental for locating features in the real world and for classification (Tehrany *et al*, 2013). Ground based work was conducted using a handheld GPS device in support of ground truthing in August 2015. The GPS device was used to record geographical coordinates of ash middens and stone-walled structures within the 49ha study area. Several coordinates were recorded starting from the centre right to the edge of each ash midden at 1m intervals. As a consequence, 39 known ash middens were recorded within the 49ha area. It is, however, important to note that field work was conducted during late spring/early summer, and not in winter as some imagery was acquired. This did not have a huge impact, if any, in the consistency of data collection as there is a rather small gap between the periods of acquiring satellite imagery and ground truthing.

### **3.2. Image Pre-processing**

Techniques including QUAC and FLAASH have been developed to halt the impacts of atmospheric interferences to avoid compromising the quality of the results from performing analyses on satellite imagery. Pre-processing an image can significantly increase the reliability of inspection. As such, images must be radiometrically and spectrally calibrated before analysis. In this case, this was done using FLAASH. FLAASH is a technique that is used to correct wavelengths in the visible through near-infrared and shortwave infrared regions ([www.harrisgeospatial.com](http://www.harrisgeospatial.com)). With its ability to support multispectral sensors, FLAASH is more appropriate for pre-processing the multispectral sensor based images used in this research. Furthermore, it contains the necessary algorithms for dealing with strong atmospheric conditions such as the presence of clouds (ENVI, 2006; Adelabu *et al*, 2014). In using FLAASH, the first step is to calibrate the images so as to extract data and create a scientific product. Calibration aims to compensate for radiometric errors from sensor defects, variations in scan angle, and system noise to produce an image that represents true spectral radiance at the sensor (ENVI, 2006; Adelabu *et al*, 2014). FLAASH was conducted on ENVi software.

### 3.3. Data analysis methods

SPOT and GeoEye imagery were processed using ENVI 5.2 software so as to classify (based on training and test samples) a number of earth surface objects using land cover classification methods. Due to the nature of the study area which does not comprise a highly differentiated land cover, 5 cover classes (Table 3) were identified. The landscape of the study area comprises mainly open dry land and vegetation. There are no surrounding features such as streams or rivers that can be included in the land cover classes. The data gathered from field work was also imported into ArcMap for visualisation, manipulation and map making.

**Table 3. Land cover classes**

<b>Land Cover Class</b>	<b>Description</b>
Ash Middens	Ash heap especially around SWS
Bare soil	Surface with no vegetation
Scattered vegetation	Mixed vegetation scattered across the landscape
Archaeological features	SWS
Road	Built-up area i.e. road

Research has shown that a number of ash middens in satellite imagery are identifiable with the naked eye as light coloured patches especially around stone walled structures (Denbow, 1979; Sadr and Rodier, 2012). Therefore, identifying ash middens on the satellite images was based on research (Sadr and Rodier, 2012) and experience gained from working with stone-walled structures and ash middens on satellite imagery, particularly Google Earth. The identified ash middens (and stone-walled structures) were then compared to the ground truth data. Identifying more or less ash middens on GeoEye and SPOT as compared to ground truth data was a step towards highlighting the differences on the performances of the two platforms as will be seen later.

### 3.3.1. Classification and Bands

Land cover classification can be supervised or unsupervised. In a supervised classification, a 'specialist' identifies training sites (areas that represent a unique land cover type) on the satellite image so as to identify classes (Sisodia *et al*, 2014). In an unsupervised classification, on the other hand, the specialists' knowledge of the identifying classes for the classification is not required (Sisodia *et al*, 2014). Instead, unsupervised classification uses spectral clusters to classify automatically. Although automated, an unsupervised classification was not selected because it suffers from producing poor accuracy from mixed pixels when working with imagery that may have classes of similar reflectance (Sisodia *et al*, 2014). Supervised classification was used in this research because it gives better accuracy when, for instance, a satellite image has the same reflectance for multiple classes (Erener, 2013; Sisodia *et al*, 2014: 1418). Supervised classification can be conducted through techniques which include Maximum Likelihood Classification (MLC), Minimum Distance and Parallepiped classification and more advanced techniques such as Support Vector Machine (SVM).

MLC and SVM were selected for this study. Referred by some as a conventional probabilistic classification technique (Foody and Mathur, 2006: 181), MLC is regarded as one of the most effective and used classifiers and it generally known for producing accurate results (Otukey and Blaschke, 2010; Aguirre-Gutierrez *et al*, 2012; Erener, 2013; Sisodia *et al*, 2014). It is a pixel-based classification technique that estimates a statistical probability based on inputs of classes created from training sites whereby a pixel is ascribed to a class it most likely belongs to (Otukey and Blaschke, 2010; Aguirre-Gutierrez *et al*, 2012; Sisodia *et al*, 2014). MLC is a parametric technique with the underlying assumption that the data assume a normal distribution (Mondal *et al*, 2012).

SVM, on the other hand, is a pattern classification method which inherently hosts a distribution-free algorithm with the potential of overcoming poor statistical estimation (Li *et al*, 2012). SVM obtains better empirical accuracy and more generalization capabilities; and more especially when working with small training sample sizes (Mountrakis *et al*, 2011; Li *et al*, 2012). Unlike MLC, SVM is a non-parametric classification technique (Mondal *et al*, 2012). MLC and SVM with their different characteristics make for a good comparison. For example,

this comparison shows whether a parametric or non-parametric approach is better for classifying archaeological features. Furthermore, studies have shown that SVM is often more accurate than MLC.

Supervised classification techniques make use of training sites which are digitized for each land cover class. The sample for the number of training sites differed for GeoEye and for SPOT. A stratified random sample technique was used to digitize the sites because it allows for the selection of a random sample within particular categories i.e. land cover classes. For GeoEye, between 50 and 70 training sites were digitized while only between 30 and 50 were digitized on the SPOT platform. The reason behind this has to do with the spatial resolution of the two platforms. GeoEye 1 has a higher spatial resolution which means one can zoom into more pixels and digitize more training sites while SPOT 5 has a lower spatial resolution meaning one cannot zoom into as many pixels as in GeoEye 1 thereby digitizing fewer training sites on SPOT 5.

A series of classifications were conducted on the imagery covering the 49ha area then tested on the wider region covered by SPOT 5 and GeoEye 1. When conducting classifications, a combination of bands was used for the different image platforms. Two major comparisons were made, one with the same bands from different satellite images and the other with different bands. GeoEye 1 and SPOT 5 have four bands each with three similar ones (Green, Red, and Near Infrared) and the last ones different from each other as shown in tables 1 and 2. Comparing the three same bands on the different platforms revealed the performance of the bands on the two distinct platforms in identifying ash middens. In the second comparison, two of the same bands from each platform combined with the last bands, making the overall combination different on the two platforms. Comparing different bands shows the impact of a blue band in GeoEye and Mid IR in SPOT 5. These combinations were as follows:

The first comparison between the same combination of bands:

- GeoEye 1: Green, Red and NIR
- SPOT 5: Green, Red and NIR

The second comparison between a different combination of bands:

- GeoEye 1: Red, Green, Blue
- SPOT 5: Red, Green, Mid IR

The measurement of reflected or emitted radiation from different surface features forms the core and foundation of remote sensing hence different surface features reflect or absorb the sun's radiation in different ways. The level of reflectance and absorption is dependent on the physical and chemical state of surface features in question such as moisture and surface roughness (Erener, 2013; Sisodia *et al*, 2014). These variations in reflectance and absorption allow for the identification of different surface features by examining their spectral reflectance patterns (and arbitrary profiles). For instance, the reflectance of green vegetation tends to be high in the in the near infrared band (Erener, 2013). For bare soil, reflectance is influenced by soil texture, and surface roughness. Vegetation will have high reflectance in NIR than bare soil.

The behaviour of these two sets (combination) of bands, as mentioned above, was compared using an arbitrary profile which refers to the pixels of any image that sit beneath a transect ([www.harrisgeospatial.com](http://www.harrisgeospatial.com)). This was carried out on the ENVi software by drawing an arbitrary profile line across an area of interest within both platforms. The area of interest was one that had a variety of classes i.e. vegetation, ash middens, SWS, soil etc. As such, the profile line went across these different classes so as to examine the pixels of each image platform when using the same bands and then different ones as can be seen in figures 2 and 3. The profile was drawn on the same areas across both GeoEye 1 and SPOT 5 image platforms on the same combination of bands and on a different combination.

### **3.3.2. Accuracy Assessment**

The most common approach for assessing accuracy of classification in remote sensing is to compare the classified land cover type with the spatial and temporal (time) data with which it corresponds, provided these are usually of high accuracy (Comber *et al*, 2012; Comber *et al*, 2013). This method is commonly known as the confusion matrix (or sometimes as the validation matrix). The confusion matrix takes into account a few accuracies, namely: overall accuracy, producer's and user's accuracy which are then used to give statistical measures of the precision and reliability of the classified information and the extent to which they are correct, or incorrect (Comber, 2012).

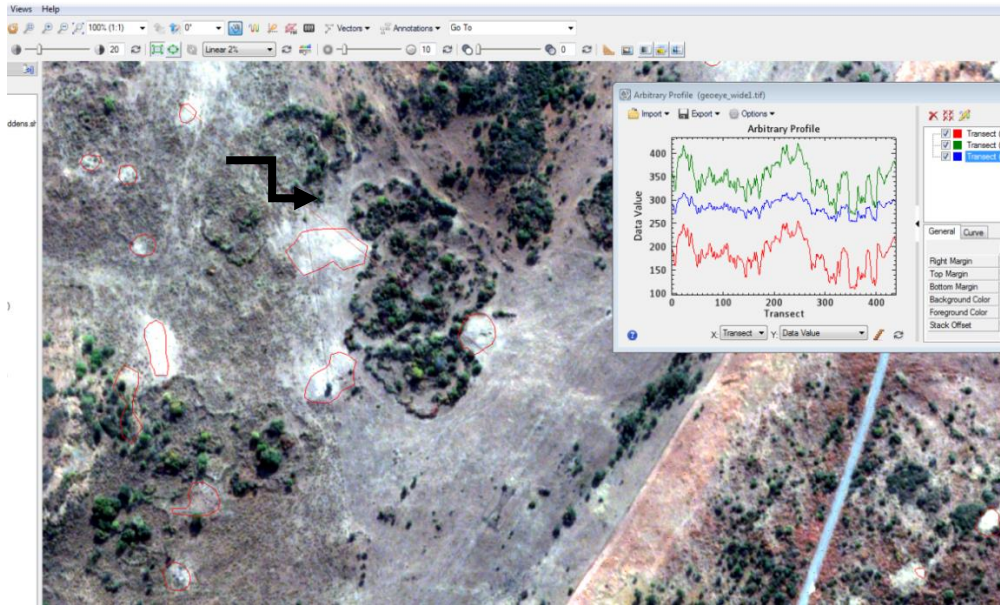


**Figure 2: An example of how an arbitrary line was drawn across the image on the GeoEye platform.**

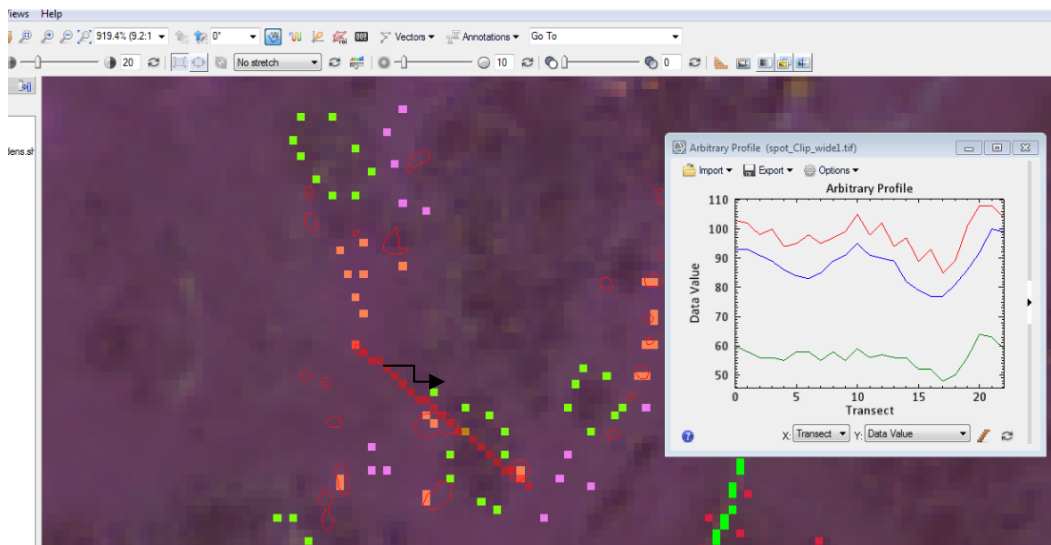


**Figure 3: An example of how an arbitrary line was drawn across the image on the SPOT platform.**

However, there are limitations to utilising this method in that the confusion matrix does not give information with regards to the spatial spread of the level of error (Comber *et al*, 2012; Comber *et al*, 2013). Furthermore, the overall accuracy provided by the confusion matrix may not be suitable for sub-regions within the land cover classes where, in reality, the accuracy levels may be higher or lower than the overall one (Comber *et al*, 2012; Comber *et al*, 2013). The confusion matrix was conducted using regions of interest (ROI) which simply refer to the geographical coordinates obtained using a handheld GPS and digitized in Google

Earth. It was conducted for MLC on SPOT 5 and GeoEye 1 and for SVM on SPOT 5 and GeoEye 1 platforms. The confusion matrix is crucial in responding to the research questions.

## **4. Results**

### **4.1. Classification**

After running supervised classification techniques – MLC and SVM – on the two platforms (GeoEye 1 and SPOT 5), the results were produced in the form of maps. The results below (figures 4 – 7) show eight maps which allow for visual comparison of the results. One can immediately spot the difference in the classification maps between SPOT 5 and GeoEye 1. SPOT 5 classification maps show less detail (larger pixels) with respect to the land cover classes as opposed to GeoEye 1 classification maps, which are more detailed. In all the images, a black outline has been overlaid to delineate known ash middens used as test middens with the 49ha study area. Similarly, a grey outline has been used to delineate stone-walled structures.

The maps are presented according to the two platforms, two classification techniques and respective band sets. The respective combination of bands is listed on the bottom right of each classified image. The first four maps (figure 4 – 5) present the classified platforms when using the same combination of bands. The second set of maps (figures 6 – 7) then presents classified platforms with the different combination of bands.

One can see from the maps (figure 4 – 7) that the black outline sits atop the bright green colour representing ash middens on the GoeEye platform more than on the SPOT platform. For example, 15 black outlines out of 39 sit on classified ash middens on SPOT 5 done with MLC and green, red and NIR. Conversely, over 25 black outlines sit on classified ash middens on GeoEye 1 using MLC and green, red, NIR. On the other hand, the grey outline is less often identified on around the pink colour representing stone-walled structures when considering both platforms and band combinations. This highlights that ash middens (black outlines) are more accurately classified than stone-walled structures (grey outlines). Furthermore, considering the lack of variety landscape of the study area (with respect to the number of land cover classes), it is fairly reasonable to suggest that other land cover features were well classified. Such features include: the road and the soil.

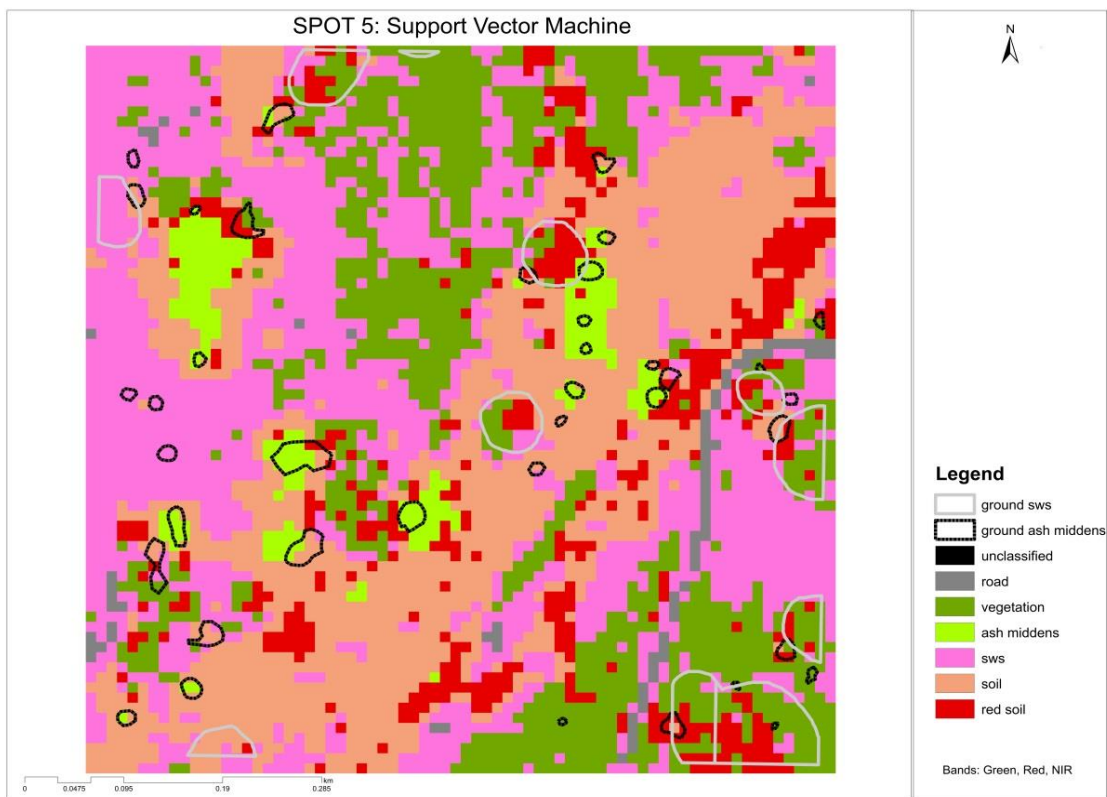
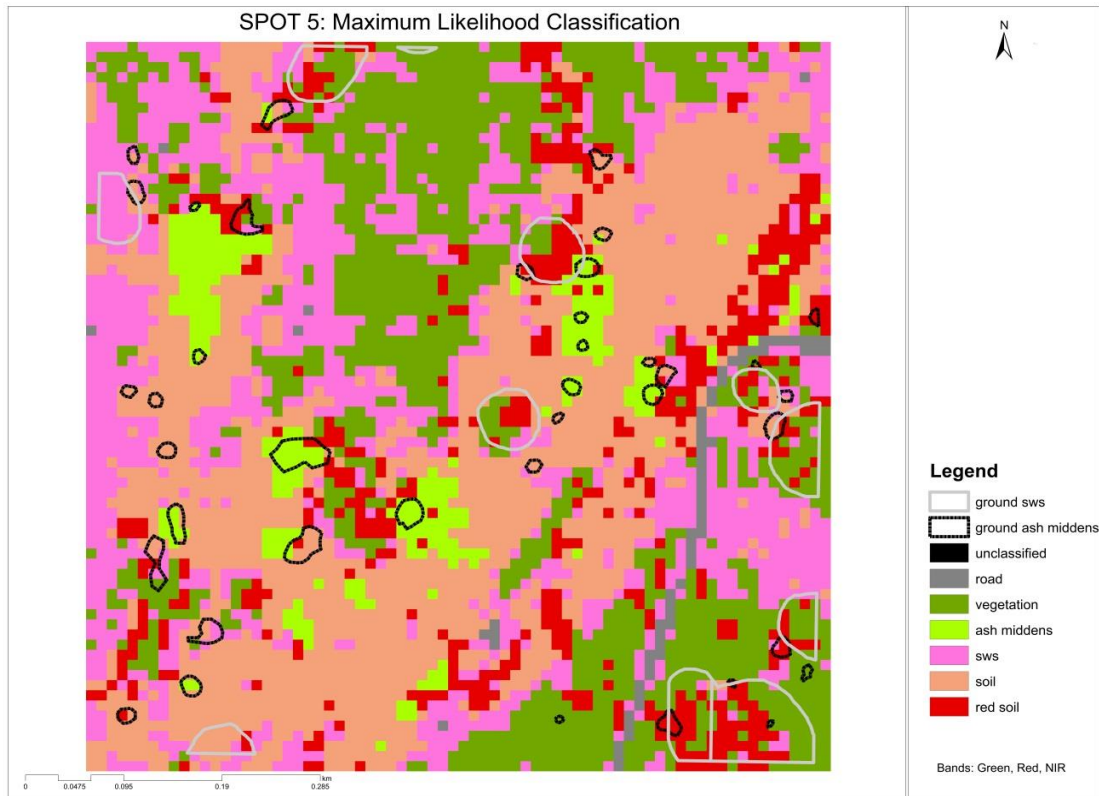


**Figure 4: Classified images from the Top: SPOT 5 MLC. Bottom: SPOT 5 SVM. Bands Green, Red, and NIR.**

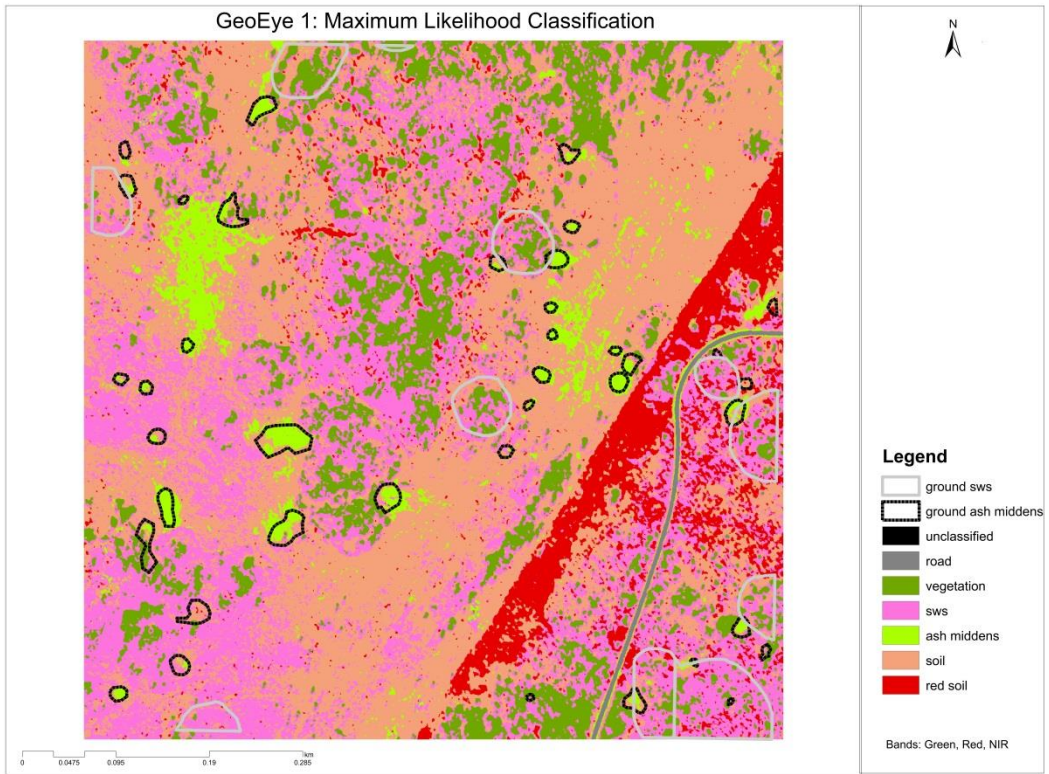


**Figure 5: Classified images from the top: GeoEye 1 MLC. Bottom: GeoEye 1 SVM. Bands Green, Red, and NIR.**

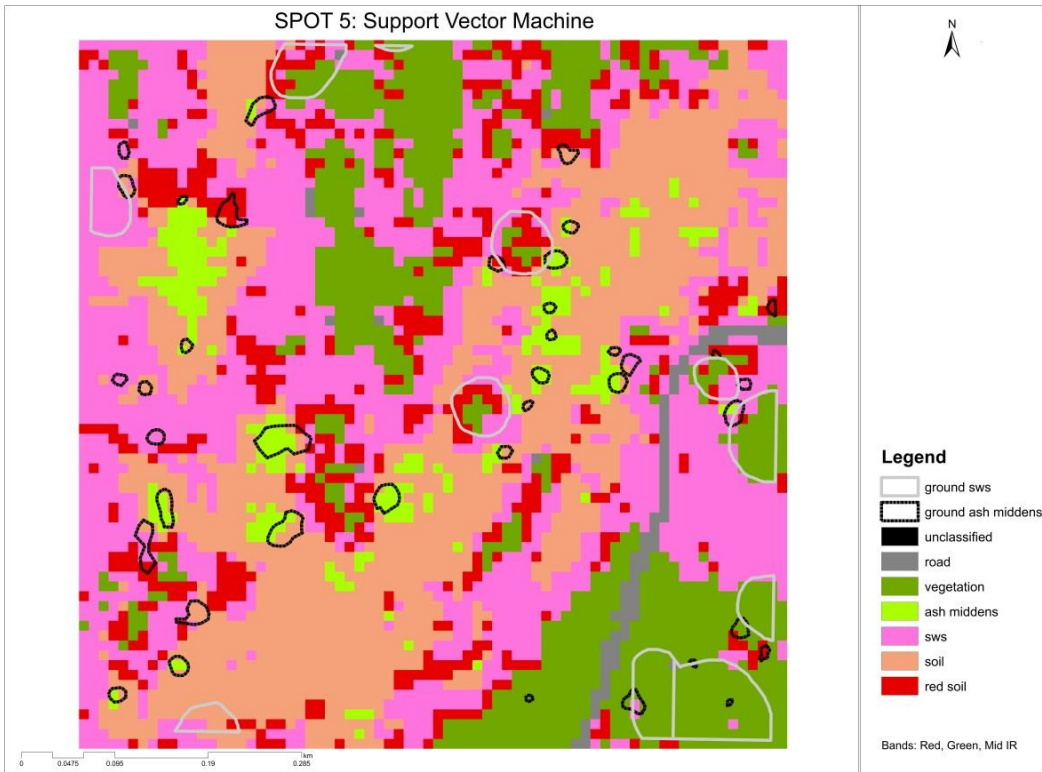
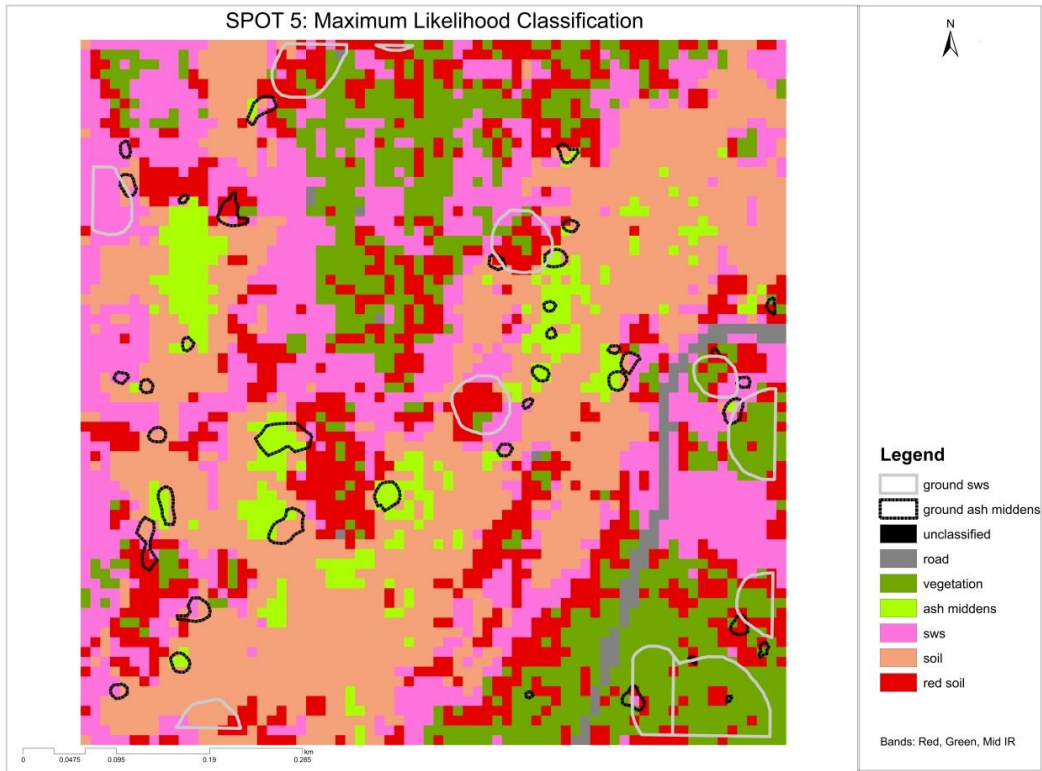


**Figure 6: Classified images from the top: SPOT 5 MLC. Bottom: SPOT 5 SVM. Red, Green, and Mid IR bands.**

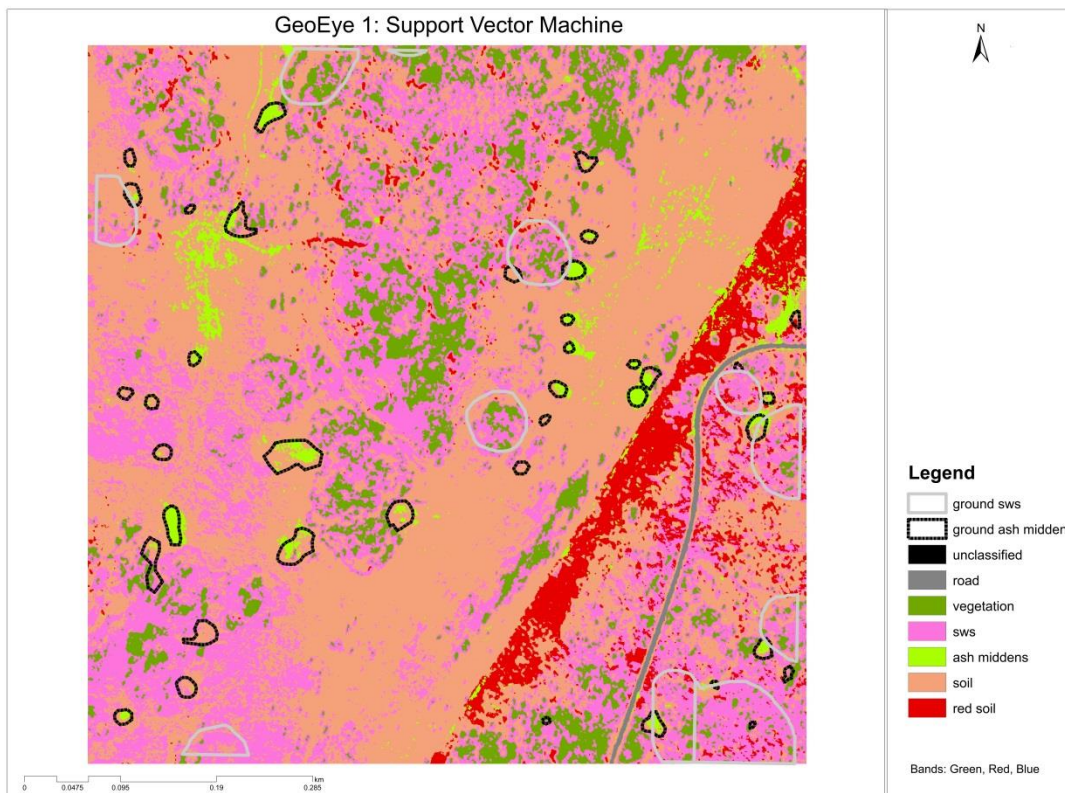
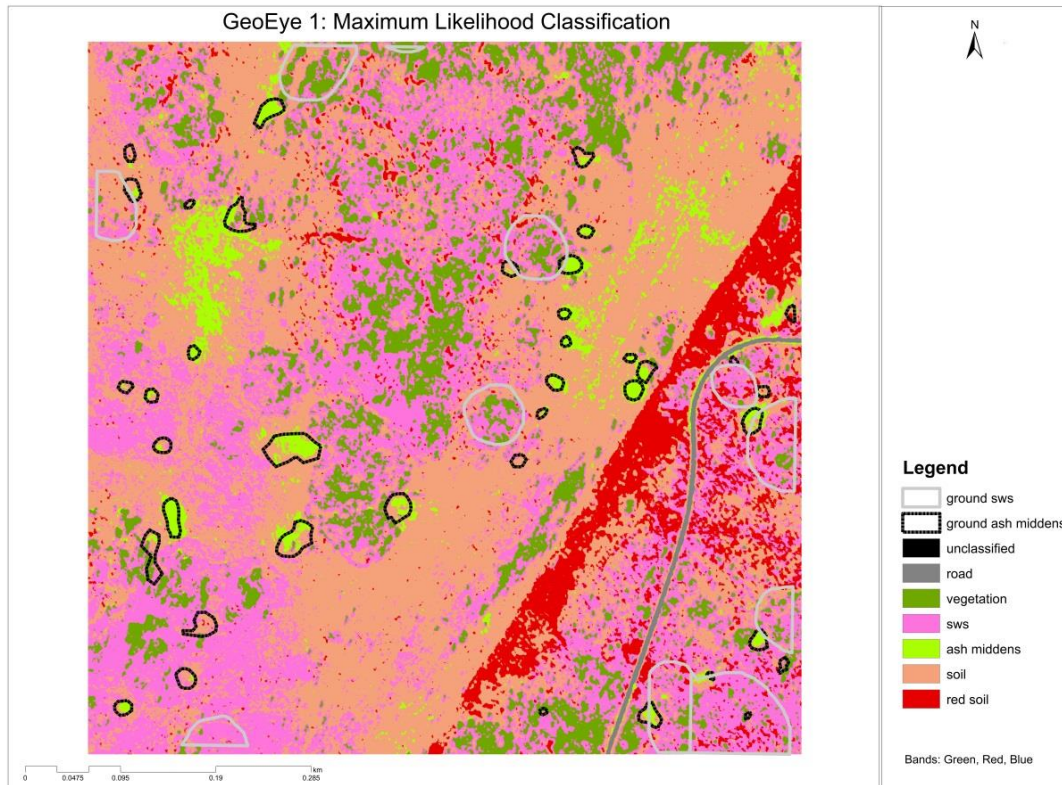


**Figure 7: Classified images from the top: GeoEye 1 MLC. Bottom: GeoEye 1 SVM. Red, Green, and Blue bands.**

## 4.2. Accuracy Assessment and Kappa Coefficient

Through using the accuracy assessment and the kappa coefficient, the accuracy of the two techniques, MLC and SVM, in classifying all the land cover classes overall and the single cover classes individually was assessed. When looking at figures 8 and 9 of the accuracy assessment results below, it is immediately apparent that the classification techniques achieved higher accuracy on the GeoEye platform as opposed to the SPOT platform. Figure 8 reports the accuracy in classifying the classes when using the combination of bands (green, red and NIR) on both platforms. When using this combination, higher results were achieved when using both MLC and SVM on GeoEye. On SPOT, both MLC and SVM were lower at 57%. Using a different combination of bands while applying the same classification techniques on the same area provided different results as shown in figure 9. Again, MLC and SVM produced higher results on GeoEye (although not as high as when using the first band combination). MLC and SVM on SPOT yielded lower results as compared to using GeoEye. As a consequence, adding Mid IR to green and red bands on SPOT increased MLC and SVM accuracy results to go higher than when using NIR with green and red.

The kappa coefficient values further coincided with the accuracy assessment results from Figures 8 and 9 which also report the kappa coefficient. The kappa ( $\kappa$ ) coefficient (equation1) serves to measure the agreement between the classification and ground truth pixels (Comber *et al*, 2012). Therefore, a kappa value of 1 represents a perfect agreement where as a value of 0 represents no agreement. Overall, there is a perfect relationship between the classification and ground truth pixels on the GeoEye platform when using either the same or different combination of bands. The same cannot be said for the SPOT platform. There is a relatively poor relationship when using the same band combinations, but a perfect relationship when using a different combination i.e. replacing NIR with Mid IR band. Nonetheless, there are some dynamics within these results that need to be considered, and these will be detailed in the discussion.

$$\kappa = \frac{N \sum_{i=1}^n m_{i,i} - \sum_{i=1}^n (G_i C_i)}{N^2 - \sum_{i=1}^n (G_i C_i)}$$

**Equation 1: Kappa coefficient**

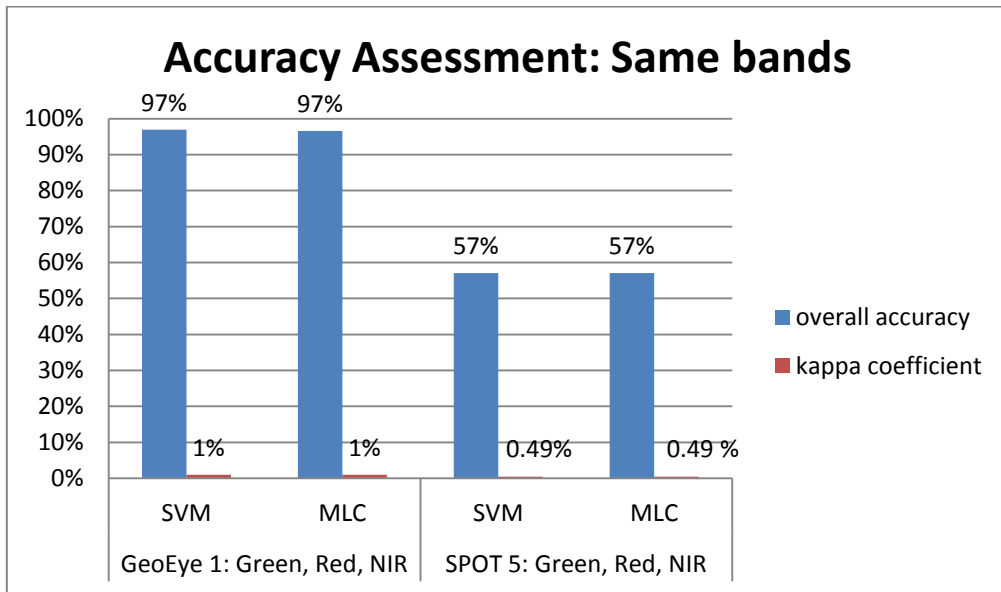


**Figure 8: accuracy assessment of the same bands (SPOT 5: Green, Red and NIR and GeoEye 1: Green, Red and NIR) on the different satellite images, SPOT 5 and GeoEye 1**

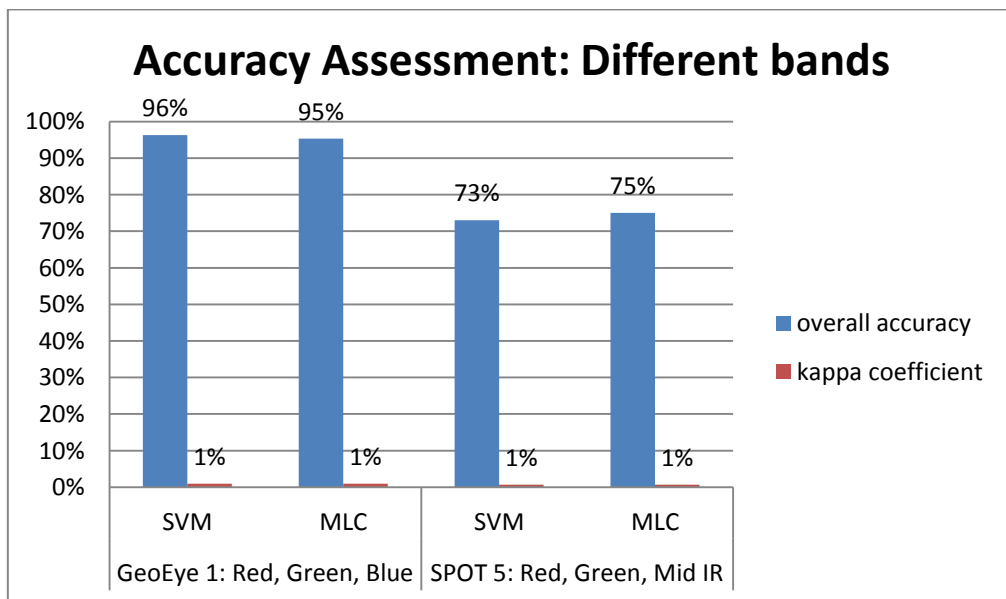


**Figure 9: accuracy assessment of different bands (GeoEye 1: Red, Green, Blue and SPOT 5: Red, Green, Mid IR) on the different satellite images, SPOT 5 and GeoEye 1.**

**4.3. User and Producer Accuracy**

In order to better articulate the reliability of the results (the overall accuracy and the kappa coefficient); the user and producer accuracies of the datasets were calculated. The user

accuracy refers to the chance that a pixel assigned as a particular land cover class in the image is really that particular class (ENVI, 2006; Adelabu *et al*, 2014). The producer accuracy refers to the chance that a particular land cover class representing an area on the ground is classified as that class ([www.harrisgeospatial.co.za](http://www.harrisgeospatial.co.za)). Both the user and producer accuracies are estimated from the full results of the accuracy assessment which is calculated in ENVI. In estimating the user and producer accuracies, the total number of classified pixels was considered. Tables (1 – 8) reporting these results are in the Appendix. All the land cover classes are included in the tables so as to show the performance of ash middens (which are highlighted) in relation to other features. The tables show that both the user and producer accuracies for ash middens are quite high. The overall accuracy of both the user and producer probabilities was higher on the GeoEye platform as opposed to SPOT. The same combination of bands – Green, Red, and NIR – yielded very high results on GeoEye 1 and SPOT 5, but the different combination of bands was not far behind on both platforms.

#### **4.4. Band Combinations**

The two band combinations of the respective platforms did not perform so differently from the above mentioned results when tested on profiles. The graphs below show the results of the arbitrary profiles, first on the same combination of bands and then on the different combination. On the one hand, GeoEye 1 profiles are very narrow because of the greater number of pixels that comes with the imagery. On the other, SPOT 5 profiles are very broad because of the fewer pixels offered by the imagery. Figures 10 and 11 show the pixels (and thereby reflectance of bands) of the selected bands (i.e. green, red and NIR on GeoEye and SPOT; replacing NIR with blue on GeoEye and with Mid IR on SPOT). There is a common pattern of peaks on areas covered by ash middens from the profiles. This is because the reflectance of ash middens at bands green, red, and NIR on both image platforms is relatively higher. It can be seen from figure 10 that the pixels of the three bands (appearing in different colours) have three relative distinct peaks that represent ash middens. Furthermore, it is worth noting that, as expected, where the profile cuts across green vegetation, NIR is higher than where the profile cuts across bare soil.

Figure 11 with the different combination of bands revealed similar results to the same band combinations in figure 10. This is because there are also three distinct peaks in the reflectances of the bands representing ash middens, and dips that represent bare soil. In figures 10 and 11, a black arrow has been used to show the peaks that represent ash middens and a grey arrow has been used to represent the relatively low signature levels of bare soil. However, the peaks representing ash middens vary as some are higher (vertically exaggerated) than others.

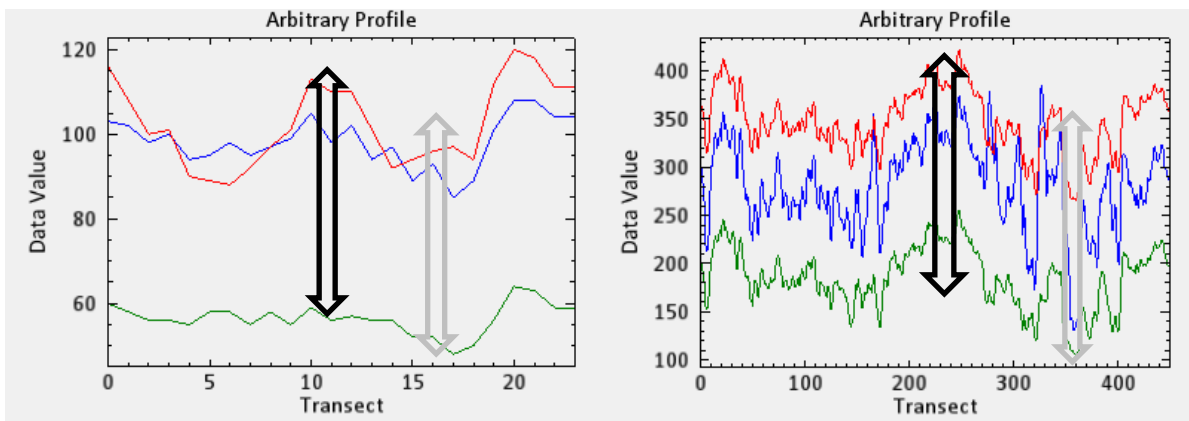


**Figure 10: left: SPOT 5. Right: GeoEye 1. Profiles from same bands on both platforms: Green, Red, and NIR.**

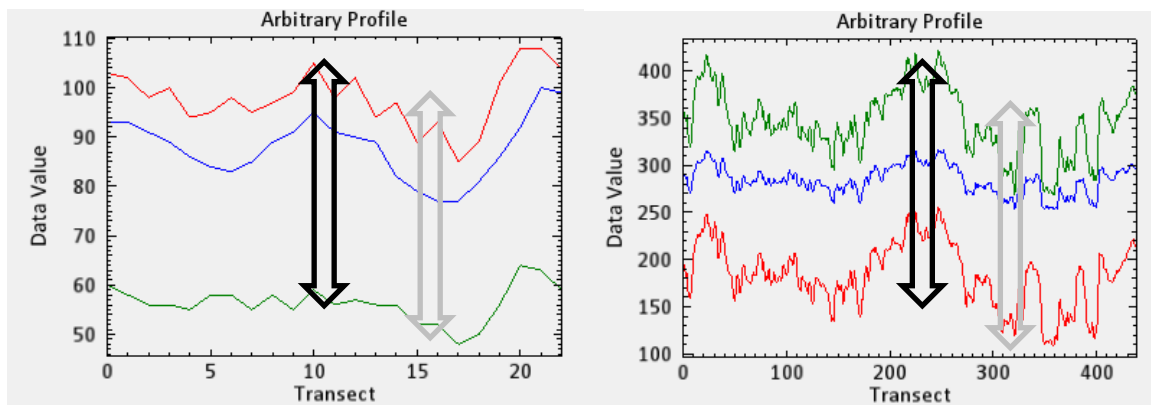


**Figure 11: profiles based on different bands on SPOT 5 and GeoEye 1. Left: SPOT 5 bands: Red, Mid IR. Right: GeoEye 1 bands: Red, Green, Blue.**

## 5. Discussion

### 5.1. Accuracy Assessment and Kappa Coefficient with respect to bands

Figure 8, showing the accuracy assessment results with the same band combinations, revealed that higher classification accuracy was achieved on the GeoEye 1 image (97% from using both MLC and SVM). MLC and SVM performed relatively poor in classifying the land cover classes (57% from both MLC and SVM). When using different band combinations between SPOT 5 and GeoEye 1 as shown in figure 9, higher classification accuracy was again obtained on the GeoEye 1 platform and lower values on the SPOT 5 platform. Nevertheless, MLC and SVM performed better on the SPOT platform using a different combination of bands (MLC: 75% and SVM: 73%). The addition of the Mid IR band green and red on the SPOT platform (thus using a different combination of bands) improves the accuracy of MLC and SVM in classifying the land cover classes. On the other hand, replacing the NIR band with the blue band on the GeoEye platform very slightly decreases the accuracy results. NIR is the optimal band for classifying the land cover classes.

The kappa coefficient values further confirmed the above mentioned preliminary conclusions. A perfect (high measure between classification and ground truth pixels) relationship between the classification and the ground truth pixels meant that the combination of bands in question were optimal. There was a perfect relationship that was achieved on the GeoEye platform when using both band combinations. Therefore, the two sets of band combinations are optimal in classifying land the specified land cover classes. This makes sense since the accuracy produced using both band combination sets was very high (above 90% for both). SPOT platform presented a different scenario. A perfect relationship was achieved when using a different band set but not when using the same band combination set. NIR is not an optimal band in classifying the land cover classes because its presence meant that there is a poor relationship between ground truth pixels and the classification. As a result, Mid IR can be deemed an optimal band on the SPOT platform based its perfect relationship. The platforms upon which the classifications were carried out must be taken into careful consideration.

## **5.2. Platforms–GeoEye and SPOT and Techniques–MLC and SVM**

The performance of the bands is influenced by the remote sensing platform. . Higher classification accuracy was achieved on the GeoEye imagery when using both the same and different combination of bands. These high accuracy results can be attributed to the higher spatial and spectral resolution of the GeoEye platform. The high resolutions mean that there

is great detail on the platform to achieve the correct classification (and a high probability of classification and ground truth pixels which is indicative of a perfect relationship). On the contrary, slightly lower accuracy results were produced when working on the SPOT imagery most likely due to the lower spatial resolution of the platform as shown in table 2. The lower spatial resolution of SPOT gives rise to relatively low classification accuracy because the pixels cover larger areas. This results in difficulties when assigning an ROI to the correct land cover class. Moreover, the lower spatial resolution may also mean that midden smaller than 10 meters in extent may be easily missed when using this imagery.

The supervised classification techniques gave somewhat unexpected results. It was expected that SVM, as an advanced technique would perform better than MLC on all platforms. This was not the case. MLC produced slightly higher accuracy (75%) on the SPOT platform when using a different combination of bands than the SVM (73%). The same can be seen from the GeoEye platform where SVM accuracy results (96%) were higher by only 1% from that of MLC (95%). Both MLC and SVM classifications had the same accuracy (97%) when classifying using same combination of bands. Although, it is important to bear in mind the influence of the GeoEye platform in yielding higher results. Both SVM and MLC performed poorly when classifying using the same combination of bands on SPOT. Overall, both SVM and MLC are good classification techniques on the GeoEye platform irrespective of the band combination and on SPOT provided that a different band combination is used. However, MLC is a better classification technique than SVM on the SPOT platform given the use bands—green, red and Mid IR but not with NIR.

### **5.3. User and Producer Accuracy**

The user and producer accuracies showed that some individual classes were better classified than others. The user and producer accuracies of all land cover classes were above 90% on the GeoEye platform when using the band combination: Green, Red, and NIR. The results (appendix) showed that there is a high probability that the pixels assigned as ash middens in the image were really ash middens on the ground. The use of the same band combination (Green, Red, and NIR) did not yield the same results on the SPOT platform as some of the land cover classes such as red soil and especially SWS were below 70% but ash middens remained high at 93%. These slightly lower accuracy values indicate a misclassification of pixels thereby mean that some areas on the ground classified as red soil are not actually red

soil, for example. On average, using a different band combination (Red, Green, and Blue) on the GeoEye platform yielded high accuracies, nothing less than 80%, almost as high as when using Green, Red, and NIR. Adding the band, MIR, on SPOT 5 saw ash midden accuracies remain high but a slight drop with red soil going below 50% and SWS staying around 65% on average. It is important to note that the addition of the blue band on GeoEye did not have a great impact on the user and producer accuracy. Adding the MIR band on SPOT did not have a great impact instead it increased the percentages of SWS and dropped that of red soil compared to NIR. According to the high user and producer accuracies, ash middens were classified more accurately irrespective of the band combination or platform as opposed to red soil, for example.

#### **5.4. Bands and Spectral Profiles**

The pixels of the platforms give rise to high reflectance of ash middens. Looking at the profile graphs on the SPOT 5 platform with the band combination green, red and NIR, it can be seen that there is a fairly higher reflectance than on the SPOT 5 platform with the band combination green, red and Mid IR. Mid IR band reduces the level of reflectance on the SPOT platform. On the other hand, similar deductions are made from the GeoEye 1 profiles. There is a slightly higher reflectance on the GeoEye 1 platform when using the band combination of green, red, and NIR as opposed red, green, and blue. The blue band reduces the level of reflectance on the GeoEye 1 platform. As a consequence, ash middens can be fairly easily located, detected and delineated with remote sensing data because they have a high reflectance, based on the image pixels, than the other earth surface features (hence the peaks on the profile graphs as shown earlier). This high reflectance could be an indication of ash middens having a distinct spectral signature and that they reflect more radiance than they absorb.

#### **5.5. Limitations**

Every study has its limitations; hindrances that might obscure the results, discussion and final interpretations of a research. In this case, the imagery from the different sensors was not acquired at exactly the same time thus slightly decreasing the comparability of the results. It is without doubt that each technique comes with certain inherent limitations. One of the major limitations of this study is the nature of the landscape (low differentiation of

land features) which makes it impossible to increase the land cover classes. Furthermore, ash that has mixed with background soil may cause confusion during the classification process. However, the spectral signature of the centre of the ash midden is invariably different from that of background soil. Nevertheless, the project was still feasible and further research using similar techniques might corroborate the nature of this project. Furthermore, only a sample of remotely sensed imagery can be examined from a relatively small area. Future studies will show how far afield the results are applicable.

## **6. Conclusion**

Using remote sensing techniques in detecting ash middens demonstrates a key step closer to saving time and money when conducting research with ash middens. The high reflectance of ash middens relative to other land cover classes has indicated that ash middens have distinct spectral signatures. The next research step could involve taking a spectrometer to the field to get readings of the spectral signatures of the respective land cover classes. Overall, the band combination of Green, Red and NIR makes the best platform on GeoEye but not very far from using Green, Red, and Blue. For SPOT, replacing the NIR with Mid IR has noticeable implications hence using the different band combinations, Green, Red, and Mid IR, made SPOT the best platform for the automated detection of ash middens. Other factors influence the process of detecting ash middens. One can say with confidence that pixels assigned as ash middens in the image were really ash middens on the ground given the high accuracy assessment results.

It is evident that certain bands are good in classifying certain classes. Having NIR on SPOT lowered the producer and accuracy results of SWS and increased those of red soil while replacing it with Mid IR increased SWS and decreased red soil. As a result, the main research questions can now be explicitly answered. The GeoEye platform is better than the SPOT platform in the detection and analysis of ash middens. This is because the spectral and high spatial resolution of GeoEye allowed for more accurate mapping of ash middens in Southern Gauteng. SVM, although advanced, is not a significantly better supervised classification technique in classifying ash middens. This means that ash middens can be well detected at medium resolution (SPOT) ideally with the use of Green, Red, and Mid IR bands. With that said ash middens can be much better detected at high multispectral resolution (GeoEye) with both band combinations. The techniques used in this study can be applied elsewhere in

southern Africa for comparison considering the material making up the ash middens; would it be the same in this area and elsewhere in southern Africa? Such a study would depend on the availability of satellite imagery, which in some regions may be hard to acquire.

## 7. References

Adelabu, S, Mutanga, O. and Adam, E., 2014: Evaluating the Impact of red-edge band from Rapideye image for classifying insect defoliation levels, *Journal of Photogrammetry and Remote Sensing*, 95, 34 – 41.

Aguirre-Gutierrez, J, Seijmonsbergen, A. C. and Duirenvoorden, J. F., 2012: Optimizing land cover classification accuracy for change detection, a combined pixel-based and object-based approach in a mountainous area in Mexico, *Applied Geography*, 34, 29 – 37.

Abrams, M. J. and Comer, D. C., 2013: Multispectral and Hyperspectral Technology and Archaeological Applications, in D. C. Comer and M. J. Harrower (eds), *Mapping Archaeological Landscapes from Space*: Springer, New York, 57-110.

Astrium., 2013: SPOT: Accuracy and Coverage combined, unknown.

Christensen, P. R, Bradfield, J. L, Hamilton, V. E, Howard, D. A, Lane, M. D, Piatek, J. L, Ruff, S. W. and Stefanov, W. L., 2000: A thermal emission spectral library of rock-forming minerals, *Journal of Geophysical Research*, 105, 9735 – 9739.

David, N., 2013: The Hidi Midden excavation: production of space and the construction of Sukur history, Report, 1-46.

Boeyens, J. C. A. and Hall, S., 2009: 'Tlokwa Oral Traditions and the Interface between History and Archaeology at Marothodi', *South African Historical Journal*, 61, 457-481.

Boeyens, J. C. A. and Plug, I., 2011: 'A chief is like an ash-heap on which is gathered all the refuse': the faunal remains from the central court midden at Kaditshwene, *Annals of the Ditsong National Museum of Natural History*, 1, 1–22.

Denbow, J. R., 1979: *Cenchrus ciliaris*: An Ecological Indicator of Iron Age Middens Using Aerial Photography in Eastern Botswana, *South African Journal of Science*, 75, 405 – 408.

Digital Globe., 2014: Geoeye 1, unknown.

Ebert, J. I., 1984: Remote Sensing Applications in Archaeology, *Advances in Archaeological Method and Theory*, 7, 293 - 362.

Erener, A., 2013: Classification method, spectral diversity, band combination and accuracy assessment evaluation for urban feature detection, *International Journal of Applied Earth Observation and Geoinformation*, 21, 397–408.

ENVI., 2006: Environment for Visualising Images. ITT Industries Inc, USA.

Fagan, B. M., 1992: *People of the Earth: An Introduction to World Prehistory*, Harper Collins, New York.

Hall, S., 2000: Forager lithics and Early Moloko homesteads at Madikwe, *Natal Museum Journal of Humanities*, 12, 33 – 50.

Hall, S., 2010: Farming Communities of the Second Millennium: Internal Frontiers, Identity, Continuity, and Change, in C. Hamilton, B. K. Mbenga, and R. Ross (eds), *The Cambridge History of South Africa Volume 1, from early times to 1885*, Cambridge University Press, Cambridge, 112 – 167.

Herold, M, Roberts, D. A, Gardner, M. E. and Dennison, P. E., 2004: Spectrometry for urban area remote sensing—Development and analysis of a spectral library from 350 to 2400 nm, *Remote Sensing of Environment*, 91, 304 – 319.

Hesse, R., 2010: LiDAR-derived Local Reliefs Models – a new tool for archaeological prospection, *Archaeological Prospection*, 17, 67 – 72.

Huffman, T. N., 2007: *Handbook to the Iron Age: the Archaeology of Pre-Colonial Farming Societies in Southern Africa*, University of Kwa-Zulu Natal Press, South Africa.

Hueni, A, Chisholm, L, Suarez, L, Ong, C. and Wyatt, M., 2012: Spectral Information System Development for Australia, *Geospatial Sciences*, unknown, unknown.

Hunt, T and Sadr, K., 2014: Inter-analyst variability in identification and classification of pre-colonial stone-walled structures using google earth, southern Gauteng, South Africa, *the South African archaeological bulletin*, 69, 87–95.

Janssen, L. L. F. and Bakker, W. H., 2004: Sensors and Platforms, in N Kerle, L. L. F Janssen, and G. C Huurneman (eds), *Principles of remote sensing*, International Institute for Geo-Information Science and Earth Observation, Netherlands, 82-126.

Keay, S. J, Parcak, S. H. and Strutt, K. D., 2014: High resolution space and ground-based remote sensing and implications for landscape archaeology: the case from Portus, Italy, *Journal of Archaeological Science*, 52, 277-292.

Lam, H, Deutsch, E. W, Eddes, J. S, Eng, J. K, King, N, Stein, S. E. and Aebersold, R., 2007: Development and validation of a spectral library searching method for peptide identification from MS/MS, *Proteomics*, 7, 655 – 667.

Lasaponara, R. and Masini, N., 2011: Satellite remote sensing in archaeology: past, present and future perspectives, *Journal of Archaeological Science*, 38, 1995 – 2002.

MacQuilkan, P. and Sadr, K., 2010: Remote Sensing of archaeological ruins: a comparison, *Position IT*, unknown, 50-51.

Maggs, T., 1976: Iron Age Patterns and Sotho History on the Southern Highveld: South Africa, *World Archaeology*, 7, 318-332.

Mason, R. J., 1986: Origins of Black People of Johannesburg and the Southern Western Central Transvaal AD350 – 1880, University of the Witwatersrand Archaeological Research Unit, Johannesburg, Occasional Paper 16.

Masaon, R. J., 1974: Background to the Transvaal Iron Age-new discoveries at Olifantspoort and Broederstroom, *Journal of the South African Institute of Mining and Metallurgy*, Unknown, 211 -216.

Mende, A, Heiden, U, Bachmann, M, Hoja, D. and Buchroithner, M., Development of a NewSpectral Library Classifier for Airborne Hyperspectral Images on Heterogeneous Environments. In Proceedings of the 7th EARSeL Workshop of the Special Interest Group in Imaging Spectroscopy, Edinburgh, UK, 11–13 April 2011.

Otukei, J, R and Blaschke, T., 2010: Land cover change assessment using decision trees, support vector machines and maximum likelihood classification algorithms, *International Journal of Applied Earth Observation and Geoinformation*, 12, 27 – 31.

Parcak, S. H., 2009: *Satellite Remote Sensing for Archaeology*, Routledge, London and New York.

Parkington, J and Hall, S., 2010: The Appearance of food production in Southern Africa 1,000 to 2,000 years ago, in C. Hamilton, B. K. Mbenga, and R. Ross (eds), *The Cambridge History of South Africa Volume 1, from early times to 1885*, Cambridge University Press, Cambridge, 63 – 111.

Renfrew, C. and Bahn, P., 1991: *Archaeology: Theories, Methods and Practice*, Thames and Hudson, London.

Sadr, K., 2012: The Origins and Spread of Dry Laid, Stone-Walled Architecture in Pre-colonial Southern Africa, *Journal of Southern African Studies*, 38, 257 – 263.

Sadr, K. and Rodier, X., 2012: Google Earth, GIS and stone-walled structures in southern Gauteng, South Africa, *Journal of Archaeological Science*, 39, 1034-1042.

Schowengerdt, A. R., 2007: *Remote Sensing: Models and Methods for Image Processing*, Elsevier, London.

Seddon, J. D., 1968: An aerial survey of settlement and living patterns in the Transvaal Iron Age: preliminary report, *African Studies*, 27, 189-194.

Sisodia, P. S, Tiwari, V. and Kumar, A., 2014: A Comparative Analysis of Remote Sensing Classification Techniques, *International Conference Advances in Computing, Communications and Informatics*, unknown, 1418 – 1421.

Taylor, M., 1979: Late Iron Age Settlements on the Northern Edge of the Vrededort Dome. M.A. Dissertation, University of the Witwatersrand, Johannesburg.

Tehrany, M. S, Pradhan, S. and Jebuv, M. N., 2014: A comparative assessment between object and pixel-based classification approaches for land-use/land-cover mapping using SPOT 5 imagery, *Geocarto International*, 4, 351–369.

White, D. A., 2013: LIDAR, Point Clouds and their Archaeological Applications, in D. C. Comer and M. J. Harrower (eds), *Mapping Archaeological Landscapes from Space*: Springer, New York, 175-210.

Woldai, T., 2004: Electromagnetic energy and remote sensing, in N Kerle, L. L. F Janssen, and G. C Huurneman (eds), *Principles of remote sensing*, International Institute for Geo-Information Science and Earth Observation, Netherlands, 49-81.

Zomer, R. J, Trabucco, A. and Ustin, S. L., 2009: Building spectral libraries for wetlands land cover classification and hyperspectral remote sensing, *Journal of Environmental Management*, 90, 2170 – 2177.

<http://www.satimagingcorp.com/> (Accessed 6 April 2015)

<http://www.sites.google.com/> (Accessed 6 May 2015)

<http://www.spotimage.com/> (Accessed 13 May 2015)

<http://www.harrisgeospatial.com/> (Accessed 23 March 2016)

<http://www.seos-project.eu/modules/remotesensing/remotesensing-c03-p02.html>

(Accessed 23 March 2016)

## 8. Appendix

Table 1: SPOT 5 MLC User and Producer accuracy. Bands: Green, Red, NIR

Class	Producer Accuracy	User Accuracy	Producer Accuracy	User Accuracy
	Percent	Percent	Pixels	Pixels
road	96.77	93.75	30/31	30/32
vegetation	60.98	75.76	25/41	25/33
<b>ash middens</b>	<b>93.55</b>	<b>87.88</b>	<b>29/31</b>	<b>29/33</b>
SWS	48.57	65.38	17/35	17/26
soil	93.55	61.7	29/31	29/47
red soil	64.52	68.97	20/31	20/29

Table 2: SPOT 5 SVM User and Producer accuracy. Bands: Green, Red, NIR

Class	Producer Accuracy	User Accuracy	Producer Accuracy	User Accuracy
	Percent	Percent	Pixels	Pixels
road	96.77	88.24	30/31	30/34
vegetation	60.98	80.65	25/41	25/31
<b>ash middens</b>	<b>90.32</b>	<b>93.33</b>	<b>28/31</b>	<b>28/30</b>
SWS	57.14	58.82	20/35	20/34
soil	70.97	56.41	22/31	22/39
red soil	67.74	65.63	21/31	21/32

Table 3: GeoEye 1 MLC User and Producer accuracy. Bands: Green, Red, NIR

Class	Producer Accuracy	User Accuracy	Producer Accuracy	User Accuracy
	Percent	Percent	Pixels	Pixels
road	100	100	58/58	58/58
vegetation	96.23	92.73	51/53	51/55
<b>ash middens</b>	<b>96.23</b>	<b>100</b>	<b>51/53</b>	<b>51/51</b>
SWS	90	93.75	45/50	45/48
soil	96.43	94.74	54/56	54/57
red soil	100	98.15	53/53	53/54

Table 4: GeoEye 1 SVM User and Producer accuracy. Bands: Green, Red, NIR

Class	Producer	User	Producer	User
-------	----------	------	----------	------

	<b>Accuracy</b>	<b>Accuracy</b>	<b>Accuracy</b>	<b>Accuracy</b>
	Percent	Percent	Pixels	Pixels
road	100	100	58/58	58/58
vegetation	94.34	96.15	50/53	50/52
<b>ash middens</b>	<b>100</b>	<b>100</b>	<b>53/53</b>	<b>53/53</b>
SWS	94	90.38	47/50	47/52
soil	96.43	96.43	54/56	54/56
red soil	96.23	98.08	51/53	51/52

Table 5: GeoEye 1 MLC User and Producer accuracy: Bands: Red, Green, Blue

<b>Class</b>	<b>Producer Accuracy</b>	<b>User Accuracy</b>	<b>Producer Accuracy</b>	<b>User Accuracy</b>
	Percent	Percent	Pixels	Pixels
road	100	100	58/58	58/58
vegetation	94.34	89.29	50/53	50/56
<b>ash middens</b>	<b>96.23</b>	<b>98.08</b>	<b>51/53</b>	<b>51/52</b>
SWS	86	91.49	43/50	43/47
soil	96.64	94.64	53/56	53/56
red soil	100	98.15	53/53	53/54

Table 6: GeoEye 1 SVM User and Producer accuracy: Bands: Red, Green, Blue

<b>Class</b>	<b>Producer Accuracy</b>	<b>User Accuracy</b>	<b>Producer Accuracy</b>	<b>User Accuracy</b>
	Percent	Percent	Pixels	Pixels
road	100	100	58/58	58/58
vegetation	96.23	91.07	51/53	51/56
<b>ash middens</b>	<b>100</b>	<b>98.15</b>	<b>53/53</b>	<b>53/54</b>
SWS	88	93.62	44/50	44/47
soil	96.43	96.43	54/56	54/56
red soil	96.23	98.08	51/53	51/52

Table 7: SPOT 5 MLC User and Producer accuracy. Bands: Red, Green, Mid IR

<b>Class</b>	<b>Producer Accuracy</b>	<b>User Accuracy</b>	<b>Producer Accuracy</b>	<b>User Accuracy</b>
	Percent	Percent	Pixels	Pixels
road	100	93.94	31/31	31/33
vegetation	70.73	64.44	29/41	29/45
<b>ash middens</b>	<b>90.32</b>	<b>90.32</b>	<b>28/31</b>	<b>28/31</b>

SWS	68.57	64.86	24/35	24/37
soil	80.65	55.56	25/31	25/45
red soil	12.9	44.44	4/31	004/09

Table 8: SPOT 5 SVM User and Producer accuracy. Bands: Red, Green, Mid IR

<b>Class</b>	<b>Producer Accuracy</b>	<b>User Accuracy</b>	<b>Producer Accuracy</b>	<b>User Accuracy</b>
	Percent	Percent	Pixels	Pixels
road	100	91.18	31/31	31/34
vegetation	56.1	67.65	23/41	23/34
<b>ash middens</b>	<b>87.1</b>	<b>93.1</b>	<b>27/31</b>	<b>27/29</b>
SWS	57.14	68.97	20/35	20/29
soil	87.1	51.92	27/31	27/52
red soil	32.26	45.45	010/31	010/22